MULTI-BASELINE INTERFEROMETRIC SAR FOR ITERATIVE HEIGHT ESTIMATION

Adam E. Robertson
Brigham Young University, MERS Laboratory
459 CB, Provo, UT 84602
801-378-4884, FAX: 801-378-6586
adam_robertson@ieee.org

Abstract — Synthetic aperture radar interferograms from properly selected multiple baselines can be combined in a manner that reduces the uncertainty in surface height estimation and avoids the downfall of traditional phase unwrapping techniques.

INTRODUCTION

Synthetic Aperture Radar (SAR) is an air or space borne imaging radar and has been used for applications that include imaging the surface of Venus and Mars, commercial topographical map generation, military reconnaissance and targeting, and measuring geological shifts on the surface of the earth. The phase difference between pairs of SAR images has been used to create interferometric images and estimate surface elevation. One of the fundamental problems is that the phase difference, or interferogram, is obtained modulo 2π. Numerous methods have been developed to unwrap the phase information and determine the absolute phase difference.

The following explores a relatively new technique for phase unwrapping that utilizes the additional phase information gained from the phase difference between multiple SAR images that have different spatial offsets, (multiple interferometric baselines). Divided into three main sections, this paper demonstrates empirical verification of interferometric phase statistics, introduces a technique for iterative height estimation, and provides an simulated example of the technique.

INTERFEROGRAM STATISTICS

Just and Bamler [1] show that the probability distribution function of the interferometric phase difference, ϕ, is,

$$\text{pdf}(\phi) = \tag{1}$$

$$\frac{1-|\gamma|^2}{2\pi}\frac{1}{1-|\gamma|^2\cos^2(\phi-\phi_o)}\times$$

$$\left\{1+\frac{|\gamma|\cos(\phi-\phi_o)\cos^{-1}[-|\gamma|\cos(\phi-\phi_o)]}{[1-|\gamma|^2\cos^2(\phi-\phi_o)]^{1/2}}\right\}, \tag{2}$$

where ϕ is the phase difference of the interferometric pair, γ is the complex correlation coefficient, and ϕ_o is defined by,

$$\phi_o = \arg\{\gamma\}. \tag{3}$$

The correlation coefficient can be calculated from the data as $|\gamma|$. The pdf of Eq. (2) is periodic in 2π. pdf(ϕ) vs ϕ for several values of $|\gamma|$ is plotted in Fig. 1. The pdf converges to a delta function as $|\gamma|$ approaches unity, and is a uniform distribution for $|\gamma| = 0$. Figure 2 shows the

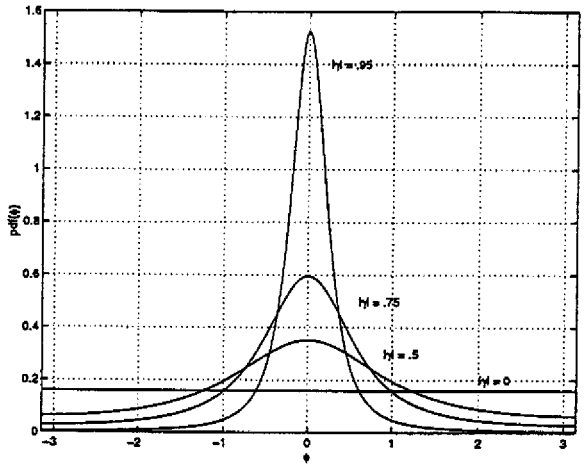

Figure 1: As the correlation coefficient approaches unity, pdf(θ) approaches a delta function. For a completely uncorrelated signal, $\gamma = 0$, the distribution is uniform. (Adapted from [1]).

experimentally determined probability distribution function. The plots come from over 10^4 phase measurements taken by YINSAR as the SNR was varied from zero to 20 dB. Both receive channels of YINSAR were connected to the same RF signal source and the signal power was varied to give different signal-to-noise ratios and correlation coefficients. The mean was subtracted from the data to center it at $\phi = 0$. Figure 3 shows the theoretical and empirically measured results of Figs. 1 and 2 together. The pdfs are in excellent agreement, verifying the accuracy of Eq. (2).

The standard deviation σ_ϕ of ϕ can be calculated as in Just and Bamler's work. The variance in the phase is dependent solely on the phase and the correlation coefficient of the data. γ, the total decorrelation, has three components: thermal noise, spatial decorrelation, and

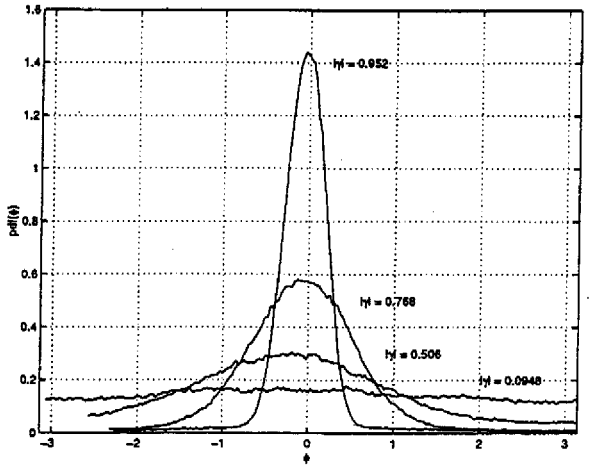

Figure 2: Empirically measured probability distribution function of the phase. Each measurement of γ used 10^4 samples. The mean was subtracted from the data to center it at $\phi = 0$.

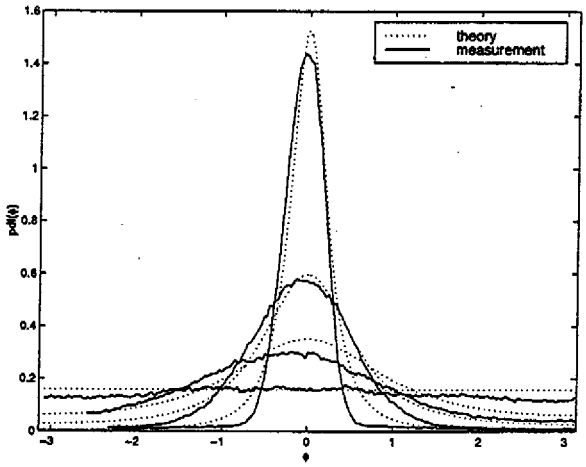

Figure 3: The theoretical and empirically measured results of Figs. 1 and 2 compared. The pdfs are in excellent agreement.

temporal decorrelation, and can be written as

$$\gamma = \rho_{spatial} \cdot \rho_{thermal} \cdot \rho_{temporal} \ . \qquad (4)$$

Assuming that the SNR for the two returns are identical the decorrelation due to thermal effects is [2, 3],

$$\rho_{thermal} = \frac{1}{1 + \mathrm{SNR}^{-1}}. \qquad (5)$$

The phase standard deviation vs signal to noise ratio is plotted in Fig. 4 using Eq. (5) where $\rho_{spatial}$ and $\rho_{temporal}$ are assumed to have unity value. Empirical

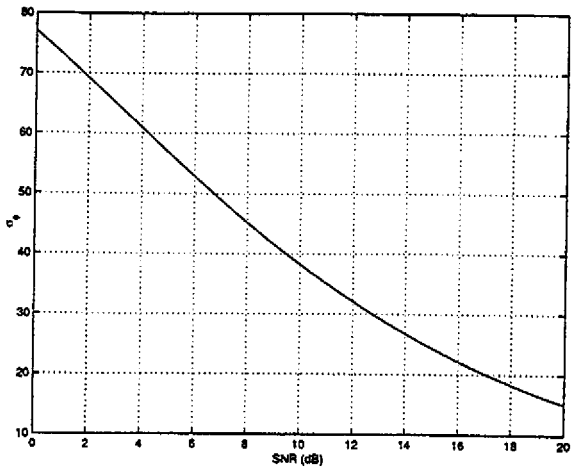

Figure 4: The phase standard deviation, σ_ϕ, vs SNR. Spatial and temporal correlation are assumed unity. The phase standard deviation falls offs sharply with the signal to noise ratio.

measured results from YINSAR have been compared to the theoretical values and are in agreement[4]. As expected, the phase standard deviation is highly dependent on the signal to noise ratio.

The estimated values for the sensitivity λ^* and for the standard deviation of the height σ_h for these two values as a function of baseline length are plotted in Fig. 5. The accuracy is as low as 20 cm for a high SNR signal using a interferometric baseline length of one meter.

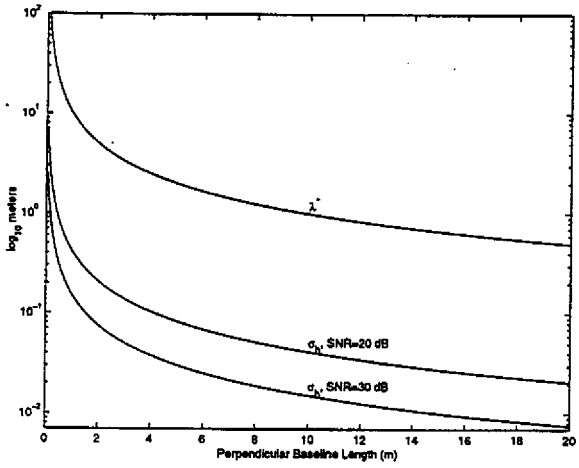

Figure 5: Sensitivity, λ^* and height standard deviation, σ_h, vs. perpendicular baseline length, $B_\perp$ for an incidence angle of $\theta = 45°$. The best (lowest) height sensitivity and standard deviation are achieved for longer baseline lengths.

Iterative Approach to Height Estimation

As stated by Corsini et. al. [5], "The main unresolved problem of this processing is still the error propagation of the noise effects". The use of multiple interferograms to determine the height may result in an increased amount of noise in the height estimate. Any linear combination of interferograms will result in an increase in the noise measurement and an unreliable estimate of the height of the scene. The following work addresses the error propagation issue and presents an application similar to projection method suggested by Xu et al. [6] to more than three antennas while minimizing the propagation of noise induced errors.

Starting with an initial estimate of the height, $\hat{h}$, with a given height standard deviation σ_h, a longer baseline with a lower σ_h and λ^* can be used to obtain a more accurate estimate of the height. The new estimate of the height is then used as an initial guess to obtain an even more accurate estimate of the height, etc. The limiting factor in the height resolution attainable by this iterative method is the critical baseline length. The following derivation follows some of the ideas presented by Xu et al. [6] and Jakowatz et al. [7].

Problem Definition and Setup

An initial estimate of the height can come from any source, e.g. a DEM or interferogram. For the case of an interferogram, if the baseline is sufficiently small for the given imaging geometry, an estimate of the height requiring minimal or no phase unwrapping can be obtained. The method presented here assumes that the initial height estimate comes from an interferogram, but can be easily adapted to an initial height estimate from other sources. Prior to explaining the method, some background and definitions are needed. Let h be the height, λ^* be the height sensitivity, ϕ be the unwrapped phase, ψ be the wrapped phase, c be the wrap count, (ϕ modulo 2π), σ_h be the standard deviation in the height, σ_ϕ be the standard deviation in the phase, and ϵ be the error in the height or phase as denoted by the associated subscript [4],

$$h_o = \frac{\lambda_s^*}{2\pi}\phi_o, \tag{6}$$

$$= \frac{\lambda^*}{2\pi}(\psi_o + 2\pi c_o), \tag{7}$$

$$\sigma_{ho} = \frac{\lambda^*}{2\pi}\sigma_{\phi_o}, \tag{8}$$

where the subscript 'o' refers to the true, or noiseless value of the parameter. Solving for c_o in Eq. (7),

$$c_o = \left(\frac{h_o}{\lambda^*} - \frac{\psi_o}{2\pi}\right). \tag{9}$$

Let the estimates of h_o, ϕ_o, and ψ_o, for interferogram i be defined,

$$\hat{h}_i = h_o + \epsilon_{hi}, \tag{10}$$

$$\hat{\phi}_i = \phi_o + \epsilon_{\phi i},$$

$$= (\psi_o + 2\pi c_o) + \epsilon_{\phi i}, \tag{11}$$

$$\hat{\psi}_i = \psi_o + \epsilon_{\psi_i}. \tag{12}$$

Note that $\epsilon_\phi = \epsilon_\psi$. The relation between the error in the height estimate and the error in the phase estimate is given by [4],

$$\epsilon_{hi} = \frac{\lambda_i^*}{2\pi}\epsilon_{\phi i}. \tag{13}$$

With the background equations fresh in mind and the definition given here a method for iteratively improving the height estimate from an initial estimate can be described.

Method for Reducing the Height Ambiguity

Iterative estimation of the height works with two interferograms at a time. Let the interferogram with the shorter baseline be denoted by the subscript 's' and the interferogram with the longer baseline be denoted by the subscript 'l'. Let the initial estimate of the height be from the small baseline, B_s, to give a height sensitivity λ_s^* with a standard deviation in the height of σ_{hs}. An initial estimate of the height from the small baseline, $\hat{h}_s$, is obtained from the phase directly or by phase unwrapping if necessary. The wrapped phase of the two interferograms are ψ_s and ψ_l, and the length of the baseline for each of the interferograms is assumed to be no more than $0.8 \times B_c$ [4]. These constraints imply the inequalities,

$$\lambda_s^* > \lambda_l^*, \tag{14}$$

$$\sigma_{hs} > \sigma_{hl}, \tag{15}$$

$$\sigma_{\phi s} < \sigma_{\phi l}. \tag{16}$$

$$\tag{17}$$

In order to reduce the ambiguity in the estimate of the height from the small baseline, the more accurate, ($\sigma_{hs} > \sigma_{hl}$), height information from the longer baseline must be used. This can be achieved by first estimating the jump count for the longer baseline using the height estimate from the shorter baseline. From Eqs. (9 - 12),

$$\hat{c}_l = \text{int}\left(\frac{\hat{h}_s}{\lambda_l^*} - \frac{\hat{\psi}_l}{2\pi}\right), \tag{18}$$

$$= \left(\frac{h_o}{\lambda_l^*} - \frac{\psi_o}{2\pi}\right) + \text{int}\left(\frac{\epsilon_{hs}}{\lambda_l^*} - \frac{\epsilon_{\phi l}}{2\pi}\right), \tag{19}$$

where int(x) rounds to the nearest integer. Note that the first term will always be an integer by definition, and is

in fact the correct jump count, (see Eq. (9)). Relating the error in height to the error in the phase through Eq. (13), $\hat{c}_l$ is,

$$\hat{c}_l = c_o + \text{int}\left(\frac{\epsilon_t}{\lambda_l^*}\right), \tag{20}$$

where ϵ_t is the total error,

$$\epsilon_t = \epsilon_{hs} - \epsilon_{hl}. \tag{21}$$

The rounding operation in Eq. (19) is performed so that when $\hat{c}_l$ is used to obtain an estimate of the height, $\hat{h}_l$, using Eq. (7), the height estimate will be congruent with the phase data of the large baseline, $\hat{\psi}_l$. Rounding to the nearest integer has several interesting implications. First of all, when the total error is less than $\lambda_l^*/2$ the effect of the error on the height estimate will be eliminated as shown in Eq. (20). When $|\epsilon_t| > \lambda_l^*/2$, the error is large enough that $\hat{c}_l$ will be different from c_o by an integer value. Accordingly, the new height estimate will be off by an integer multiple of λ_l^*. By Eqs. (12 - 13) and (20 - 21), the new height estimate is,

$$\begin{aligned}\hat{h}_n &= \frac{\lambda_l^*}{2\pi}(\hat{\psi}_l + 2\pi\hat{c}_l), \\ &= \frac{\lambda_l^*}{2\pi}(\hat{\psi}_l + 2\pi c_o) + \lambda_l^* \text{int}\left(\frac{\epsilon_{hs} - \epsilon_{hl}}{\lambda_l^*}\right), \\ &= \hat{h}_l + \lambda_l^* \text{int}\left(\frac{\epsilon_t}{\lambda_l^*}\right). \end{aligned} \tag{22}$$

The probability of an error and its effect on the height estimate must be carefully evaluated. If the effect of the integer error in the estimate $\hat{c}_l$ can be reduced or removed it will be possible to obtain an estimate of the height, $\hat{h}_n$, that is better than the initial estimate, $\hat{h}_s$.

The pdf for ϵ_t is Gaussian [4]. Assuming that ϵ_s and ϵ_l are uncorrelated, the standard deviation of the total error is,

$$\sigma_{ht} = \sqrt{\sigma_{hs}^2 + \sigma_{hl}^2}. \tag{23}$$

The probability distribution function of the error is,

$$p(\epsilon) = \frac{1}{\sigma_{ht}\sqrt{2\pi}} \exp\left(-\frac{\epsilon^2}{2\sigma_{ht}^2}\right). \tag{24}$$

The probability that $\hat{c}_l \neq c_o$, resulting in an error in the new height estimate is,

$$\begin{aligned} P_{error} &= P\left(|\epsilon_t| > \frac{\lambda_l^*}{2}\right), \\ &= 2\int_{\frac{\lambda_l^*}{2}}^{\infty} p(\epsilon)d\epsilon, \\ &= 1 - 2\text{erf}\left(\frac{\lambda_l^*}{2\sigma_{ht}}\right), \end{aligned} \tag{25}$$

where the error function is defined,

$$\text{erf}(x) = \frac{1}{\sqrt{2\pi}}\int_0^x \exp(-x^2/2)dx. \tag{26}$$

The probability distribution function of the new height estimate, $\hat{h}_n$, is illustrated in Fig. 6. The new pdf is a discretely sampled Gaussian distribution. For example, when $\lambda_l^*/2 < \epsilon_t < 3\lambda_l^*/2$ an error of 1 will occur in $\hat{c}_l$, which is equivalent to an error in the phase estimate of 2π. By Eq. (22) this is equivalent to an error of λ_l^* in the height estimate, $\epsilon_{hn} = \lambda_l^*$. The pdf, mean, and variance

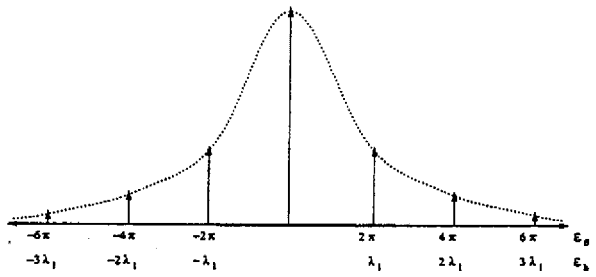

Figure 6: The probability distribution function for the error in the new height estimate. An error in estimating the jump count will always be an integer value. The error in the phase estimate is an integer multiple of 2π and the error in the height estimate is an integer multiple of λ_l^*.

are,

$$\begin{aligned} \text{pdf}(\epsilon_{\phi n}) &= \delta(0)P_{correct} + \sum_{n=1}^{\infty}[\delta(2n\pi) + \delta(-2n\pi)] \times \\ &\quad \frac{1}{2}P\left(\frac{(2n-1)\lambda_l^*}{2} < \epsilon_t < \frac{(2n+1)\lambda_l^*}{2}\right) \end{aligned} \tag{27}$$

$$\begin{aligned} \mu_{\phi n} &= E(\epsilon_{\phi n}), \\ &= \int_{\infty}^{\infty} \epsilon_{\phi n} \cdot f(\epsilon_{\phi n})d\epsilon_{\phi n}, \\ &= 0, \\ \sigma_{\phi n}^2 &= E\left[(X-\mu)^2\right], \\ &= \int_{\infty}^{\infty}(x-\mu)^2 f(x)dx, \\ &= \frac{8\pi^2}{\sqrt{2\pi}}\sum_{n=1}^{\infty} n^2 \int_{(2n-1)\frac{\lambda_l^*}{2\sigma_{ht}}}^{(2n+1)\frac{\lambda_l^*}{2\sigma_{ht}}} \exp(-t^2)dt. \end{aligned} \tag{28}$$

Assuming a finite bandwidth on the noise, the value of σ_{hn} can be determined from Eq. (28) using a finite summation. When $\sigma_{hn} < \sigma_{hs}$ the height estimate of $\hat{h}_n$ is better than $\hat{h}_s$ and $\hat{h}_n$ can be used as a new height estimate with a standard deviation of σ_{hn} and a sensitivity of λ_l^*. By iteratively proceeding with smaller and smaller λ_l^* to achieve better estimates of h_o a height sensitivity limited by the baseline length giving complete spatial decorrelation can be achieved.

Baseline Length Selection for Iterative Height Estimation

Of great significance is the choice of baseline lengths. The baseline length is inversely proportional to the sensitivity of the interferometer [4]. If the value for λ_l^* is too large, ($\lambda_l^* \approx \lambda_s^*$), σ_{hl} will also be large resulting in an increased probability of error, $\sigma_{ht} = \sqrt{\sigma_{hs} + \sigma_{hl}} \gg \sigma_{hs}$. If the value for λ_l^* is too small compared to λ_s^* the probability of error will be unacceptably large, resulting in a poor height estimate, (See Eq. (25)). Thus, there exists an optimal value for the baseline lengths.

The probability of error is used to determine the appropriate baseline length for improving the height estimate. To reduce the chance of a bad estimate of c_l a low probability of error must be chosen. The appropriate probability of error is dependent on the type of filter that will be used as described in the following section. Given a desired P_{error}, the first step in finding the ideal longer baseline length is to determine the correlation coefficient from. Assuming no temporal decorrelation,

$$\gamma = \left(\frac{1}{1+\mathrm{SNR}^{-1}}\right)\left(1 - \frac{|B_\perp| R_y}{\lambda R_o \tan(\theta)}\right). \qquad (29)$$

Alternatively, for real data the complex correlation coefficient, γ can be calculated directly from the data. $\sigma_{\phi s}$ and σ_{hs} can then be calculated from $|\gamma|$. Equation (25) and the inverse error function are used to calculate λ_l^*,

$$\lambda_l^* = 2\sigma_{ht}\mathrm{inverf}\left(\frac{1-P_{error}}{2}\right). \qquad (30)$$

Because σ_{ht} is dependent on σ_{hl} which is a function of λ_l^*, Eq. (30) must be solved numerically. The final step in finding the desired longer baseline, B_l, is to use [4],

$$B_l = \frac{\lambda R_o}{\lambda_l^*}[\sin(\alpha) - \cos(\alpha)\tan(\alpha - \theta)]. \qquad (31)$$

When the look angle and the baseline tilt are identical $B_i\lambda_i^*$ is a constant,

$$B_l = \frac{B_s \lambda_s^*}{\lambda_l^*}. \qquad (32)$$

This method is iteratively used to find larger and larger baselines based on the desired probability of error and the accompanying standard deviation and baseline length until the upper limit of (0.5 - 0.8) B_c is achieved, or the maximum number of antennas is reached.

Filters for Iterative Height Estimation

In order to iteratively achieve smaller and smaller σ_{hi} values for each new $\hat{h}_i$ it is beneficial to use a filter to reduce the phase noise. The errors in $\hat{h}_n$ will be integer multiples of λ_l^*. Two common and easily implemented filter are mentioned here. More advanced filters may result in lowering the number of interferograms and/or the length of the baselines required to achieve a given quality for the height estimate.

One filter for removing the effect of the errors is a spatial average. Jakowatz [7] demonstrated that a 3×3 pixel average effectively reduced the number of errors. His result is not congruent with the input phase, ψ_s. By applying a congruency operator after the filtering operation the error can often be further reduced and the resulting $\hat{h}_f$ has a σ_{hf} significantly less than the σ_{hn} of Eq. (28). A spatial filter will reduce the standard deviation of the height estimate according to,

$$\sigma_{hf}^2 = \frac{\sigma_{hn}^2}{N}, \qquad (33)$$

where N is the number of pixels averaged and a uniform weighting is assumed. (Note: spatial averaging, or Multi-Look processing, is commonly used to decrease the noise and speckle effects in SAR images). On the negative side, the spatial averaging reduces the image resolution and the sharpness of true discontinuities in the image.

Another filter for removing the integer multiples of λ_l^* in the height estimate is the median filter. Because the errors are large compared to the rate at which the surface topography is changing, the median value of a 3×3 pixel region results in very little smoothing or loss of sharpness and avoids averaging in the errors as in the spatial average. The median filter serves to reduce the height standard deviation to some degree, but the effect can not be analytically determined due to the non-linear nature of the filter, and must be measured empirically. Congruency with the underlying data can be forced, but will result in a standard deviation equivalent to that of the underlying data. Constraining the estimate to be congruent does not necessarily reduce the standard deviation of the height estimate.

The type of filter that is used is dependent on the desired result and the underlying data. In an mountainous environment with rapid and continual elevation changes, the median filter may not be the ideal choice and the mean filter may provide the best estimate of the height. In an urban environment a median filter is superior due to it's edge preserving qualities. Much of the decision on the filter type and the chosen probability of error is qualitative in nature. The ability of a filter to remove error in the height estimate determines the probability of error that is chosen, and therefore, the optimal baseline lengths for a given geometry.

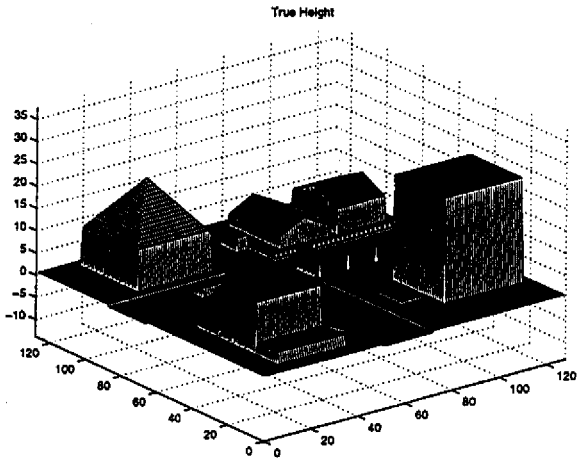

Figure 7: True Height of the Simulated Urban Scene

MULTI-BASELINE INTERFEROMETRY

A synthetic urban scene is illustrated in Fig. 7. Georectification and the removal of the nominal flat earth induced phase difference are assumed. It is also assumed that data with an SNR of 10 dB is available at all points in the image. The examples shown here assume the imaging geometry given in Table 1, similar to that of YINSAR.

Table 1: Interferometric Imaging Geometry

Parameter	Symbol	Value
Nominal Platform Height	H	300 m
Radar Wavelength	λ	0.03 m
Pixel Size	R_y	0.6 m
Baseline Length	B	1 m
Baseline Tilt	α	45°
Incidence Angle at Beam Center	θ	45°

Fig. 7 gives the true height of the simulated scene. Each ground pixel represents 0.6×0.6 meters. The tallest building in the image is eight stories tall, assuming 3 m equals one story. The building with a pyramid shaped roof reaches a total height of 21 meters and the smaller building in the foreground is four stories tall with 1 story side wings and steps leading up to the building (steps are not clearly visible from the perspective shown). In the upper corner of the image a one story and two story house is simulated with 2 m high fence posts placed along the road. The road is .3 meters below the level of the buildings, the size of a large curb. A 3 m high truck and a 2 m high car are visible in the streets as well as a 6 m high 1 pixel wide bar representing a stop light support. 6 m street lights are present between the tallest building and the houses.

Table 2: Baseline length selection for $P_{error} = 0.05$. The measured standard deviations represent the result of a using a 3×3 median filter to eliminate errors in the height estimate.

B	λ^*	$\sigma_{measured}$	σ_h
0.3	30.3	3.4	3.4
0.906	10	0.636	1.23
2.44	3.73	0.309	0.541
5.21	1.74	0.215	0.307
8.61	1.06	0.185	0.217

For a comparison of standard phase unwrapping with multi-baseline techniques, consider Fig. 8, the simulated height estimate from a single baseline using Flynn's minimum discontinuity phase unwrapping method [8]. Phase unwrapping algorithms can not determine the height of regions of the image isolated by phase discontinuities, and assume the step size is less than λ^*, the value causing a 2π phase change. When the phase is continuous, such as for the slanted roofs and the steps leading up to the building with side wings, the phase is properly unwrapped.

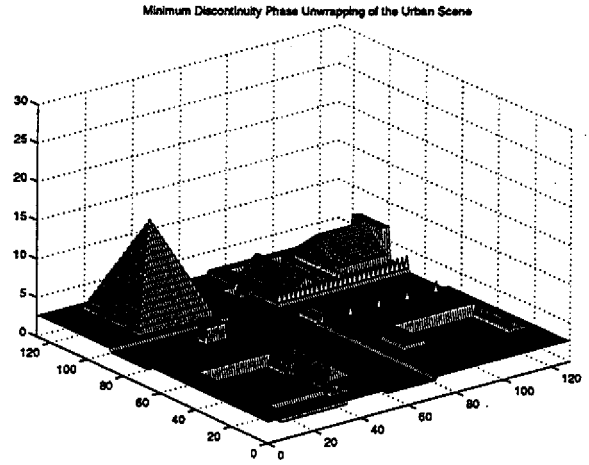

Figure 8: Height estimate of an urban scene using a single interferometric baseline and Flynn's minimum discontinuity phase unwrapping method. For simplicity, noiseless phase measurements were used. Phase unwrapping assumes any step discontinuity to have a magnitude of less than λ^*.

The example in this paper uses the median filter with P_{error}, the probability of having a phase wrap error, at 0.05. Figure 9 is a cross section of the scene in Fig. 7. The true height, initial estimate of the height, and the estimate from the second and fourth iterations are shown.

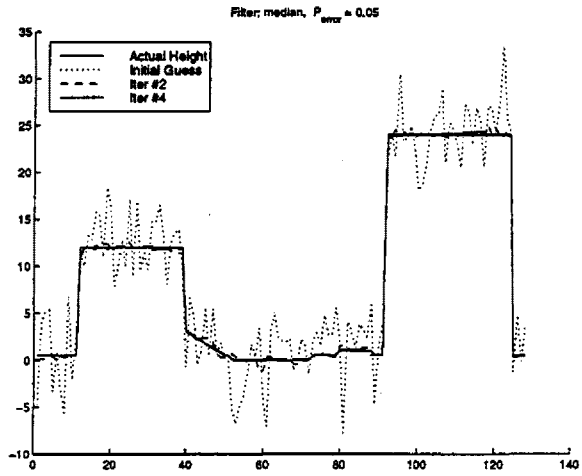

Figure 9: Cross section of the urban scene showing the iterative improvement in the height estimation using the median filter. The baseline lengths were chosen according to Table 2.

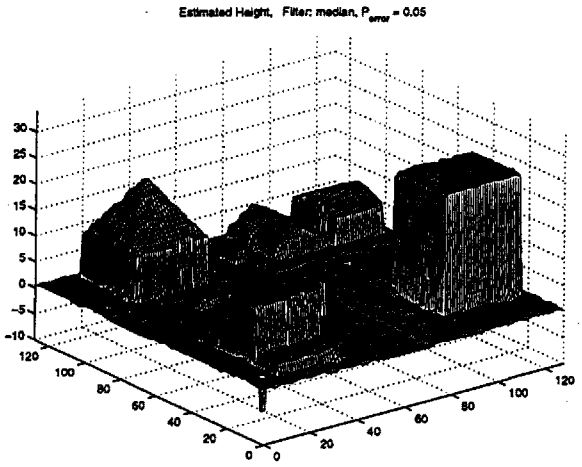

Figure 10: Final height estimate of the scene using a 3×3 median filter. The resulting standard deviation is listed in Table 2.

Table 2 shows the baseline lengths for each iteration, the height λ^* which causes a 2π phase change for that baseline, $\sigma_{measured}$, the measured height accuracy for the simulation, and σ_h, the theoretical height accuracy for that baseline alone. $\sigma_{measured}$ values are lower than the theoretical primarily because of the filtering step. The results in the table are intuitively pleasing. For each iteration the new value for λ^* is roughly half of the previous value. As the baseline length increases the spatial decorrelation increases and the percent change in λ^* correspondingly decreases. Figure 10 illustrates the result

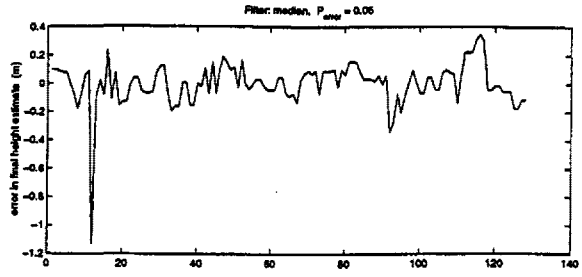

Figure 11: The error in the final height estimate for a cross section of the urban scene using $P_{error} = 0.05$ and a median filter.

of the iterations performed using the baselines in Table 2. As expected the light poles and fence which were only one pixel wide are completely removed by the 3×3 pixel median filter. The stop light support pole is undetectable for the same reason. The sides of the buildings all have a slight slope due to the filter. The final plot of Fig. 11 is the error in the final height estimate for the cross section shown in Fig. 9.

CONCLUSION

The additional phase information obtained from properly selected multiple baselines can be used to reduce the uncertainty in estimating surface elevation. An iterative technique is used so that filters can eliminate errors in the jump count for each interferogram absolute phase estimation. Phase unwrapping is not necessary to determine surface height from a set of SAR images.

*

REFERENCES

[1] Dieter Just and Richard Bamler. Phase statistics of interferograms with applications to synthetic aperature radar. *Applied Optics*, 1994.

[2] E. Rodriguez and J. M. Martin. Theory and design of interferometric synthetic aperture radars. *IEEE Proceedings*, 1992.

[3] Howard A. Zebker and John Villasenor. Decorrelation in interferometric radar echoes. *IEEE Transactions on Geoscience and Remote Sensing*, 1992.

[4] Adam E. Robertson. Multi-baseline interferometric sar for iterative height estimation. Master's thesis, Brigham Young University, 1998.

[5] G. Corsini, M. Diani, and F. Lombardini. Reduction of the phase-unwrapping drawbacks by the three-antenna interferometric sar system. *International Geoscience and Remote Sensing Symposium*, 1997.

[6] Wei Xu, Ee Chien Chang, Leong Keong Kwoh, Hock Lim, and Wang Cheng Alice Heng. Phase-unwrapping of sar interferograms with multi-frequency or multi-baseline. *International Geoscience and Remote Sensing Symposium*, 1994.

[7] Charles V. Jakowatz Jr., Daniel E. Wahl, and Paul A Thompson. Ambiguity resolution in sar interferometry by use of three phase centers. *Proceedings of the SPIE The International Society for Optical Engineering*, 1996.

[8] T.J. Flynn. Two-dimensional phase unwrapping with minimum weighted discontinuity. *Journal of the Optical Society of America A*, 1997.